DESIGN AND DEVELOPMENT OF ENGINE FUEL CONSUMPTION MEASURING DEVICE

Shuangfei ZHANG[1], Zongzheng MA[2]*, Yong CHENG[3], Jianjun NIE[4], Saifei WANG[5], Qingzhong YAN[6]

To address the issues of low precision and unstable measurements in traditional fuel consumption meters under conditions of frequent load fluctuations and unstable engine output power, a novel fuel consumption measuring device has been designed. The mechanical structure design of this device primarily include the design of a pressure stabilizing system, the configuration of a measuring oil cup, and the selection of a nozzle. The control system design involves sensor selection and the development of the control program. Actual test results indicate that the measurement error of this device is less than 1.5% compared to the CMFD010 high-precision fuel consumption detection instrument, thereby achieving the expected design requirements.

Keywords: fuel consumption measurement, measuring oil cup, pressure stabilization system, control system.

1. Introduction

The fuel consumption measuring device can monitor the engine's operational status, display the vehicle's current fuel consumption in real-time, and assist drivers in adjusting their driving habits to improve fuel economy. The operating conditions of engines in engineering machinery are complex, and fuel consumption exhibits a pulsating pattern, increasing the difficulty of accurate measurement [1-2]. Converting pulsating fuel supply into a stable fuel supply and achieving precise fuel consumption measurement is of significant importance for real-time monitoring of engine fuel consumption [3].

Currently, the primary methods for measuring diesel engine fuel consumption include the gravimetric method, volumetric method, carbon balance method, electronic injection pulse width method, and ultrasonic method [4]. The gravimetric method offers high measurement accuracy but features a complex structure and is only suitable for stable operating conditions [5]. The volumetric method, exemplified by the turbine flow meter, typically employs blade rotor

[1] School of mechatronics Engineering, Zhongyuan University of Technology, China
[2]* Prof, School of Mechanical Engineering, Henan Institute of Engineering, China, e-mail: zongzhengma@haue.edu.cn (corresponding author)
[3] Prof, School of Energy and Power Engineering, Shandong University, China
[4] School of mechatronics Engineering, Zhongyuan University of Technology, China
[5] School of mechatronics Engineering, Zhongyuan University of Technology, China
[6] Jinan Reinuo Power Technology Co, Ltd. China

structures and gear structures, with the rotor count proportional to the flow rate. However, this method can have measurement errors due to increased viscosity when fuel temperature decreases and is sensitive to pressure fluctuations in the fuel line [6]. The carbon balance method is based on the law of conservation of mass, with measurement accuracy depending on the precision of emission measurements, but its high equipment cost limits its widespread adoption [7]. The electronic injection pulse width method, tailored for electronically injected engines, uses ECU fuel injection signals for cumulative fuel consumption calculation, but injector characteristics are significantly affected by engine speed variations [8]. The ultrasonic method utilizes the principle of changes in ultrasonic pulse velocity in the fluid medium's downstream and upstream directions to calculate fuel consumption based on fuel flow rate, but its measurement accuracy is influenced by fuel quality, fuel pipe wall thickness, and the positioning of ultrasonic probes [9].

To enhance the accuracy of engine fuel consumption measurement, a fuel consumption measuring device that converts pulsating fuel supply into a stable fuel supply has been designed. This device is characterized by its simple structure, low cost, and broad applicability. Using this device instead of traditional fuel consumption meters can reduce the impact of frequent fuel line fluctuations on measurement accuracy, which is of great significance for evaluating engine performance and tracking fuel consumption statistics.

2. Basic structure of fuel consumption measuring device

The basic structure of the fuel consumption measuring device is illustrated in Fig. 1. Based on the direction of fuel flow, the device comprises two main sections: the fuel tank circuit and the engine circuit [10]. The fuel tank circuit includes the fuel tank, filter, fuel pump, regulator box, and pressure regulating valve. Its function is to guide fuel through the filter into the regulator box via the fuel pump, establish stable pressure within the regulator box, and ensure consistent nozzle flow rates when the solenoid valve opens. The engine circuit comprises the measuring oil cup, inlet pipe, return pipe, and heat dissipation device, providing fuel to the engine and ensuring its smooth operation.

These circuits are interconnected via a constant speed tube. Fuel is dispensed to the engine through the bottom oil outlet of the measuring oil cup, while the engine return oil is cooled by the heat dissipation device and cycles back into the measuring oil cup via the return port. A solenoid valve regulates different flow rate calibration nozzles, filling the measuring oil cup accordingly. The volume of fuel passing through the nozzle determines engine fuel consumption. For engines of varying power levels, precise fuel consumption measurement is achieved by using appropriately calibrated nozzles.

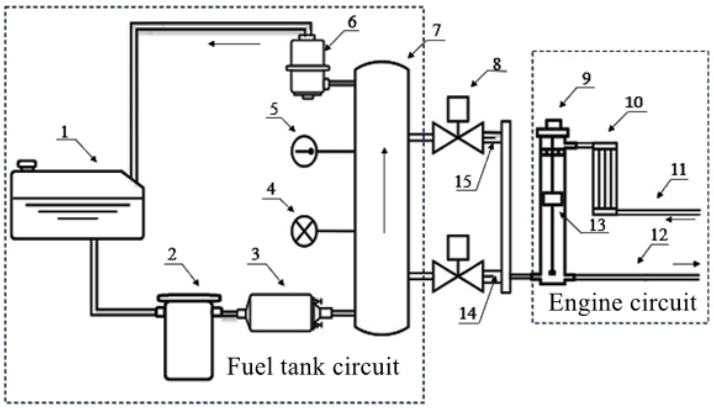

1. Fuel tank 2. Filter 3. Fuel pump 4. Pressure sensor 5. Temperature sensor 6. Pressure regulating valve 7. Pressure stabilization box 8. Solenoid valve 9. Measuring oil cup 10. Cooling device 11. Engine return oil port 12. Engine oil inlet 13. Level sensor 14. Nozzle A 15. Nozzle B

Fig. 1. System structure diagram

3 Fuel consumption measurement principle

3.1 Measurement principle of cumulative fuel consumption

During engine operation, the liquid level sensor float in the oil cup descends with fuel consumption, and two calibration nozzles, A and B, are used to replenish the oil in the measuring oil cup. As shown in Fig. 2, when the float drops to the F_L position, nozzle A refills the measuring oil cup. When the fuel injection quantity from nozzle A exceeds the engine's fuel consumption, the float will rise to the F_H position. At this point, the solenoid valve closes, and the opening time T_1 of nozzle A is recorded. When the fuel injection quantity from nozzle A is less than the engine's fuel consumption, the float will drop to the F_{min} position. The opening time T_1 of solenoid valve A is recorded, and nozzle B is opened. At this point, both nozzles A and B simultaneously refill the measuring oil cup until the float rises to the F_H position. Subsequently, nozzles A and B close, and the opening time T_2 of nozzle B is recorded.

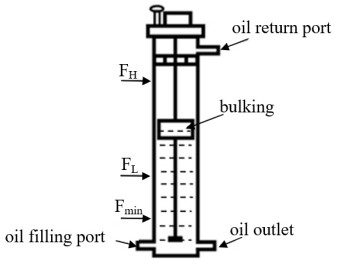

Fig. 2. Schematic diagram of measuring oil cup

When only Nozzle A is opened, the flow rate in the uniform tube is recorded as Q_A, and the fuel injection volume is recorded as V_A, where:

$$V_A = Q_A \times T_1 + \Delta V_A \tag{1}$$

Similarly, when both nozzles A and B are opened simultaneously, the flow rate in the uniform tube is recorded as Q_{AB}, and the fuel injection volume is recorded as V_{AB}, where:

$$V_{AB} = Q_A \times (T_2 - T_1) + Q_{AB} \times T_2 + \Delta V_{AB} \tag{2}$$

ΔV_A and ΔV_{AB} are the system errors caused by the mechanical characteristics of the solenoid valve. In the experiment, the cumulative error principle is used for measurement. The timing control solenoid valve is used to start and stop. By comparing the nozzle flow difference between continuous opening for 400 seconds and starting and stopping once every 20 seconds for a total of 400 seconds, the fuel increase per nozzle start-stop cycle is determined. The calculation method is shown in Eq. (3):

$$\Delta V = \frac{\sum_1^{20} V_1 - V_2}{(20-1)} \tag{3}$$

where V_1 is the flow volume of the nozzle when it is intermittently opened (mL), and V_2 is the flow volume when the nozzle is continuously opened (mL).

ΔV_A and ΔV_{AB}, (mL) can be obtained by measuring the increase in flow when nozzle A is opened alone and when both nozzles A and B are opened simultaneously. According to Eqs. (1) - (3), the total fuel consumption of the engine is:

$$V_{sum} = \sum_0^{N_1} V_A + \sum_0^{N_2} V_{AB} + \Delta V_H \tag{4}$$

where, N_1 and N_2 are the number of times nozzle A opens alone and the number of times nozzles A and B open simultaneously.

3.2 Measurement principle of average fuel consumption

Average fuel consumption refers to the amount of fuel consumed by the engine over a specific time period. Two methods are used: constant volume measurement and timing measurement. In constant volume measurement, the duration of continuous fuel supply from the full oil cup volume is calculated. Specifically, t_1 is recorded when the floating block rises to the F_H position, and t_2 when it drops to the F_L position. The calculation method for average fuel consumption is represented by Eq. (5):

$$V_{Ave} = \frac{H \times \pi \times d^2}{4 \times (t_2 - t_1)} \tag{5}$$

To enhance measurement accuracy, marking points such as F_1, F_2, F_3, etc., can be added to the measuring oil cup. In the timing measurement method, a constant interval time is maintained, and the distance ΔH that the floating block falls within this period is measured. This allows calculation of the average fuel consumption. Both methods offer high measurement accuracy. Longer

measurement durations or greater fuel consumption result in higher accuracy in average fuel consumption measurement.

4. Design and selection of important components of fuel consumption measuring device

4.1 Design of the pressure stabilization box

According to the Bernoulli equation in the ideal state of fluid mechanics and the principle of uniform tube measurement, disregarding the influence of liquid level height, the flow velocity and pressure at both ends of the nozzle are denoted as v_1, v_2, p_1 and p_2, respectively.

$$\frac{v_1^2}{2}+\frac{p_1}{\rho}=\frac{v_2^2}{2}+\frac{p_2}{\rho} \tag{6}$$

when $v_1=0$:

$$p_1-p_2=\Delta p=\rho\frac{v_2}{2} \tag{7}$$

$$Q_V=KAv_2=K\frac{\pi d^2}{4}\sqrt{2\frac{\Delta p}{\rho}} \tag{8}$$

$$V_T=Q_VT=K\frac{\pi d^2}{4}\sqrt{2\frac{\Delta p}{\rho}}T \tag{9}$$

Where ρ is the fuel density in g/mL, v is the flow velocity at both ends of the nozzle in m/s, p_1 and p_2 are the pressures at both ends of the nozzle in Pa, Δp is the pressure difference between the two ends of the nozzle in Pa, Q_V is the nozzle flow in mL/s, and K is the flow coefficient of the nozzle, which is related to the length, inner diameter, and material of the nozzle. A is the nozzle cross-sectional area in mm^2, d is the inner diameter of the nozzle in mm, t is the time in s, and V_T is the volume of fuel flowing through in mL.

From the above equation, it can be seen that when the fuel density and nozzle specifications are determined, the nozzle flow velocity is only related to the pressure difference Δp. To reduce the influence of pressure fluctuations on nozzle flow velocity, and considering the body space and relevant designs [11-12], the buffer partition inside the regulator box can effectively improve pressure stability. The designed pressure stabilization box has an effective internal volume of 1.5 L. To verify the design effectiveness, numerical analysis was used to compare the structures of the pressure stabilization box with and without the baffle. During the analysis, the inlet boundary condition was set to a volumetric flow rate of 200 L/h, the return oil port boundary condition was set to a static pressure of 0.4 MPa, and the boundary conditions for the two nozzles were set to a static pressure of 0.1 MPa. The calculation results are shown in Fig. 3 and 4.

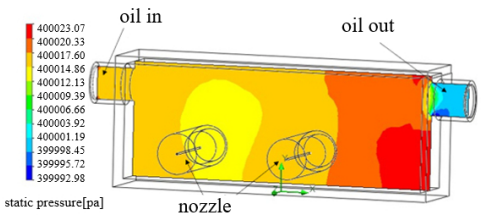

Fig. 3. Schematic diagram of cross-sectional pressure without buffer baffle

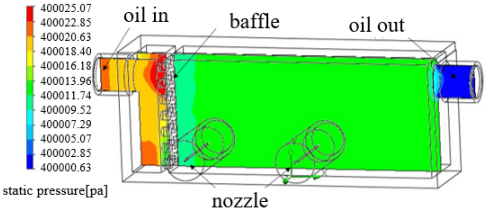

Fig. 4. Schematic diagram of cross-sectional pressure with buffer baffle

According to the analysis results, the maximum pressure difference inside the box without a buffer partition is 14 Pa, while the maximum pressure difference in the right part of the box with a buffer partition is 4 Pa. With the buffer partition added, the liquid at the oil inlet enters the right side of the box evenly through the small hole in the partition, effectively reducing pressure fluctuations on the right side. The oil inlet and return port are placed at the upper end of the pressure stabilizer, with the nozzle installed at the same height on the side of the stabilizer. This arrangement minimizes the influence of pressure changes due to height differences between the two nozzles.

4.2 Design of measuring oil cup

The measuring oil cup is a key component in the measuring system, and its size affects the volume of the equipment and the operation of the solenoid valve. If the oil cup volume is too large, the equipment becomes bulky. Conversely, if the volume is too small, the solenoid valve will start and stop frequently. To enhance the resolution of liquid level detection, the size of the measuring oil cup is designed considering the size of the floating block of the liquid level sensor. The inner diameter of the measuring oil cup is 40 mm, the height is 250 mm, and the floating block of the liquid level sensor moves within a range of 150 mm. The oil return port at the upper end of the measuring oil cup is designed as a semi-conical surface, allowing the oil to flow along the cup wall. This design effectively eliminates oil return foam, reduces liquid level fluctuations, and enhances sensor measurement stability. The physical diagram of the designed measuring oil cup is illustrated in Fig. 5.

Fig. 5. Measurement of oil cup physical picture

4.3 Selection of pressure regulating valve

The pressure regulating valve's function is to maintain the pressure within the pressure stabilizing box. When the pressure in the stabilizing box exceeds the

combined force of the spring pressure and vacuum gas pressure, the diaphragm arches upwards, opening the regulator valve. Fuel then flows back to the tank through the ball valve via the oil return port, reducing the internal pressure. Once the pressure decreases to the cut-off level set by the regulator, the ball valve closes, maintaining the internal pressure at the set value. The pressure regulating valve ensures a constant pressure difference between the stabilizing box and atmospheric pressure, eliminating pressure pulsations from the fuel pump and fluctuations caused by nozzle operations.

Currently, common fuel pressure regulating valve specifications include 0.3MPa, 0.35MPa, and 0.4MPa. Test comparisons indicate that higher-specification pressure regulating valves result in smaller pressure fluctuations and more stable pressure within the stabilizing box. Therefore, a 0.4MPa pressure regulating valve was selected. When the nozzle opens, the pressure difference (Δp) at both ends of the nozzle remains constant at 0.4MPa.

4.4 Fuel pump selection

The fuel pump drives the fuel flow, transporting it through the filter to the regulator box, where pressure is established. Thus, the output pressure of the fuel pump must exceed the pressure regulator's set pressure. Consequently, the FP015-5 external fuel pump was chosen. The fuel pump has a rated flow of 200L/h and a rated output pressure of 0.5MPa. Installing a one-way valve at the fuel pump outlet ensures the engine closes the oil circuit after stopping, prevents oil return in the stabilizing system, quickly establishes stable pressure upon engine restart, and reduces start-up time.

4.5 Selection of nozzle

For engines with varying power outputs, selecting an appropriate nozzle to meet the fuel supply demand is essential. Specifically, a single nozzle should fulfill the engine's average fuel consumption under normal conditions, while the combined fuel injection of two nozzles should exceed the engine's maximum power demand. Given an engine rated at 220 kW, the fuel consumption calculation formula indicates the required fuel flow as:

$$Q \geq \frac{P \times B}{H \times \rho} = \frac{220\text{kw} \times 230\text{g/kwh}}{3600\text{s} \times 0.83\text{g/mL}} = 17.67\text{mL/s} \qquad (10)$$

where Q is the fuel flow (mL/s), P is the engine power (kW), and B is the fuel consumption coefficient (230 g/kWh). Based on Eq. (10), the basic parameters of the selected nozzle are shown in Table 1.

Table 1

Basic nozzle parameters

Specification	Outer diameter(mm)	Inner diameter(mm)	Total length(mm)	Flow(mL/s)
A	1.28	0.84	50	10
B	1.05	0.75	50	8

5 Design of the control system

The control system primarily consists of a temperature sensor, pressure sensor, liquid level sensor, solenoid valve module, power management module, 4G DTU module, data storage module, and display module. The overall hardware schematic is illustrated in Fig. 6.

5.1 Overall scheme design

The control system uses an STM32 microcontroller as the main control unit, which, through pressure sensors, temperature sensors, and level sensors, measures the internal pressure of the pressure stabilization box, the oil temperature, and the liquid level in the oil measuring cup [13]. The main control chip controls the start and stop of the solenoid valve based on the output signal from the level sensor. It stores the sensor data in a local storage chip and simultaneously displays the data on the screen via a serial port. Additionally, a 4G-DTU is utilized to upload the data to a cloud server or a remote computer terminal.

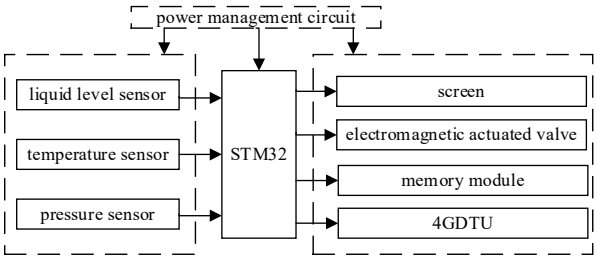

Fig. 6. The overall structure of the control system

5.2 Design of the sensor data acquisition circuit

The current-mode sensors significantly enhance the system's resistance to interference. Hence, the temperature, liquid level height, and pressure sensors employed in this system operate in current-mode, generating an output signal of 4 ~ 20mA. Since the microcontroller cannot directly read current signals, a sampling resistor converts the current signal into a voltage signal, which is then amplified by an operational amplifier to produce a voltage range of 0 ~ 3.3V. The signal processing circuit design is depicted in Fig. 7.

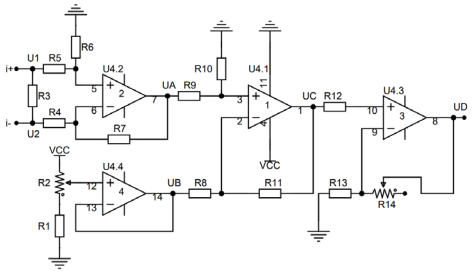

Fig. 7. Signal processing circuit

Operational amplifiers 1 and 2 form a differential amplifier circuit, operational amplifier 3 serves as a co-directional amplifier, and operational

amplifier 4 acts as a voltage follower. During operation, the signal processing module initiates data calibration by applying a standard 4mA current to the input, adjusting resistor R2 to achieve 0V at node D. Subsequently, a standard 20mA current is applied, and resistor R14 is adjusted to set node D voltage to 3.3V.

5.3 Design of the electromagnetic valve drive module circuit

The measuring equipment employs two 24V direct-acting normally closed solenoid valves for controlling the start and stop of the nozzle. Due to the high current during solenoid valve startup, a dual-channel low-voltage driver rated up to 40V/20A drives the field-effect transistor STN4186, serving as a switch for the solenoid valve. To mitigate current-induced effects during solenoid valve operation, the IR4427 dual drive chip is employed to amplify and isolate the signal. The schematic diagram of the designed solenoid valve drive is depicted in Fig. 8.

5.4 Design of the display module

As an important means of human-computer interaction, the display screen can dynamically showcase the system's operating status in real time, facilitating testers in observing experimental phenomena and recording the experimental process. The SDWb043S43C configuration screen selected for this test system exchanges data with the host via RS485 serial communication. This screen features rich control functions, a simple user interface, a wide power supply voltage range, low cost, and strong compatibility. Additionally, it allows for the customization of the serial port protocol through software, simplifying the development process. Fig. 9 shows the schematic diagram of the RS485 serial communication circuit.

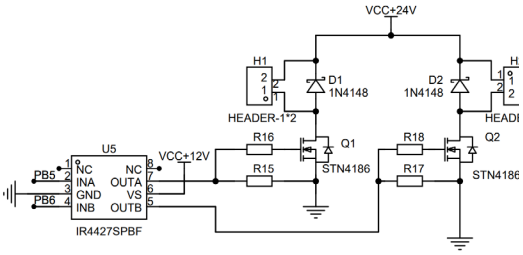

Fig. 8. Solenoid valve drive circuit

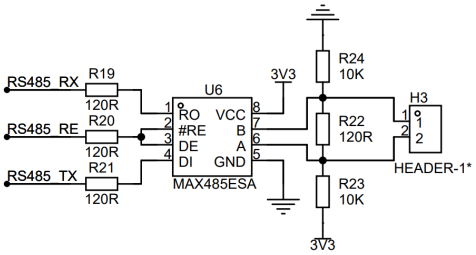

Fig. 9. RS485 serial communication schematic diagram

5.5 Design of the software

To achieve accurate fuel consumption measurement, the system must simultaneously count the number of solenoid valve openings and calculate the duration of each opening. Hence, the system connects the solenoid valve's output control pin, external interrupt pin, and timer input capture pin to enable concurrent recording of both the duration and frequency of solenoid valve openings. Fig. 10 illustrates the workflow of the control system. Upon power-up, the main program initializes each sensor, records the initial liquid level height, and determines the appropriate solenoid valve based on this height. Opening the solenoid valve generates a rising edge signal, triggering an external interrupt. The external

interrupt program accumulates the number of solenoid valve openings and starts the timer for counting. Closing the solenoid valve generates a falling edge signal, which triggers the timer interrupt after the timer captures it. The interrupt function reads the timer count, which represents the duration the solenoid valve remained open.

Upon solenoid valve closure, the system calculates the flow rate corresponding to the current temperature and time, accumulating data according to Eq. (3) and (5) determines that the fuel consumption value calculated during the timer interrupt function represents the engine's average fuel consumption. After executing the interrupt function, the program returns to the main function to save and display the data on the screen. Simultaneously, the 4G-DTU transmits data to the cloud, enabling remote viewing and analysis by a computer.

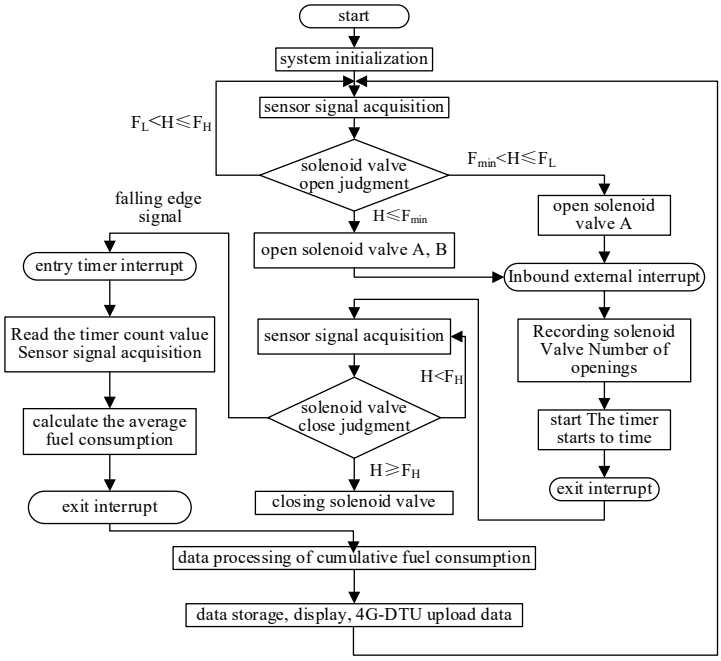

Fig. 10. Working flow chart of control system

6 Accuracy experiment

To test the reliability and measurement accuracy of the designed fuel consumption detection device, a large excavator with a model of 22 tons and a maximum output power of 220 kW was chosen as the test subject. The designed fuel consumption measurement device is compared with the CMFD010 Coriolis mass flowmeter produced by American High Precision Company [14]. The basic parameters of the flowmeter are shown in Table 2:

Table 2

Basic parameters of CMFD010 mass flowmeter

Parameter	Description	Parameter	Description
Rated flow mass(kg/h)	0-65	Zero drift(kg/h)	0.00166
Maximum flow mass(kg/h)	90	Precision(%)	0.12
Response time(s)	<0.1	Reproducibility(%)	0.05

In the test process, the designed fuel consumption measurement device and the CMFD010 mass flowmeter are connected in series to the excavator's fuel circuit according to the connection mode shown in Figure 11. The excavator performs typical operational cycles including soil excavation, lifting rotation, unloading of soil materials, and no-load return. Each test cycle lasts for 15 minutes, and experimental data from both measurement devices are recorded at six different operational speeds. The measurement results are shown in Table 3.

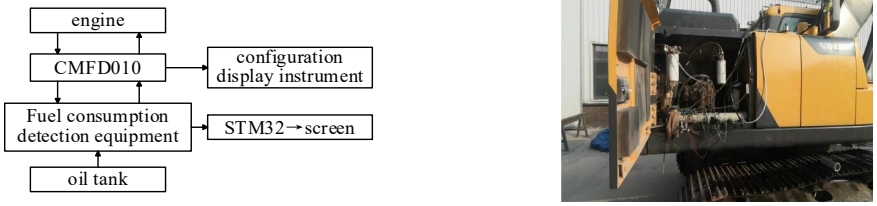

(a) Test pipeline connection diagram (b) Test pipeline real vehicle connection diagram

Fig.11. Experimental verification of fuel consumption accuracy measurement

Table 3

Experimental data

Speed(rpm)	Data of this device(mL)	Data of CMFD010(mL)	Data(%)
1208	3654	3599	1.49
1416	3552	3590	1.34
1715	3497	3464	0.94
1875	3366	3395	0.86
1966	3449	3403	1.33

The measurement results indicate that the maximum deviation of the fuel consumption measurement device designed in this paper compared to the CMFD010 standard fuel consumption measuring instrument is within 1.5%. This demonstrates high measurement accuracy of the device, coupled with its simple structure and low cost. It can effectively substitute traditional fuel consumption meters for engine fuel consumption detection.

7 Conclusions

The pressure stabilization box achieves the transition from pulsating fuel supply to stable supply through a buffer partition structure. It maintains a constant pressure difference at both ends of the nozzle, ensuring a consistent nozzle flow rate. The device measures fuel consumption by calculating the switching time of the solenoid valve. After testing and data calibration, the device can be applied to large machinery such as ships, trucks, and cranes, where precision requirements are

moderate. So it could be used in different circumstances where measurement accuracy is not the main goal but it could not be used as a laboratory instrumentation due to its 1.5% deviation compared to the standard measuring instrument CMFD010 fuel consumption meter.

REFERENCES

[1]. *D. J. Liu, H. Wang, Z. Q. Zheng, et al.* Energy and loss Analysis of Different Combustion Modes of Internal Combustion Engine. Combustion Science and Technology, **vol. 27**, no. 5, Sept. 2019, pp. 529-538.

[2]. *Q. S. Zhang.* Influence of tractor Drive System on its performance and Fuel consumption and Experimental study. Agricultural Mechanization Research, **vol. 46**, no. 2, Sept. 2019, pp. 249-254+259.

[3] *Z. Q. Wei, W. Z. Gao, J. Wu, et al.* Effects of oil cut-off and reflux destocking Strategy on engine Fuel Consumption and shafting Torsional Vibration. Chinese Internal Combustion Engine Engineering, **vol. 40**, no. 3, Sept. 2019, pp. 94-101.

[4] *X. F. Huang, Y. F. Peng.* Application Research of Vehicle Fuel Consumption Parameter Measurement Method. Computer Simulation, **vol. 28**, no. 11, Sept. 2011, pp. 339-342.

[5] *G. C. Wang, L. T. Jiang.* Discussion on calibration items and methods of carbon balance fuel consumption meter. Metrology Technology, no. 7, Sept. 2019, pp. 71-73.

[6] *C. Yin, X. L. Lin, Z. B. Guo.* Experimental Analysis of fuel Consumption Measurement and flow Resistance Characteristics of turbine flow Sensor. China Test & Technology, **vol. 45**, no. 10, Sept. 2019, pp. 78-83.

[7] *M. D. Fang, H. Y. Zheng.* Automobile Fuel consumption Measurement Method based on carbon balance Method. Automotive Engineering, no. 3, Sept. 2003, pp. 295-297+294.

[8] *X. Y. Wu, S. Y. Luo, H. W. Huang.* Design and Verification of FSAE Engine Intake Correction System. Journal of Nanjing University of Science and Technology, **vol. 38**, no. 2, Sept. 2019, pp. 234-240.

[9] *X. L. Fu, Z. G. Yang, X. J. Wang.* Application of Multisim in fuel injection pulse width detection. Journal of University of Electronic Science and Technology of China, no. 1, Sept. 2016, pp. 43-46.

[10] *X. F. Liu, Z. L. Li, X. K. Chen, et al.* Design of Continuous Fuel Consumption Instrument for Engine Bench Test. Modern Manufacturing Engineering, no. 6, Sept. 2020, pp. 31-36.

[11] *F. L. Liao, Y. L. Xu, B. F. Zu, et al.* Application of porous media Model in Numerical Simulation of Engine Inlet. Chinese Internal Combustion Engine Engineering, **vol. 37**, no. 5, Sept. 2016, pp. 165-169.

[12]. *X. Liu, Y. D. Deng, K. Zhang, et al.* Experiments and simulations on heat exchangers in thermoelectric generator for automotive application. Applied Thermal Engineering, **vol. 71**, no. 3, Sept. 2014, pp. 364-370.

[13] *W. Duan, B. N. Niu, F. X. Xie, et al.* Application of Capacitive liquid level Sensor in Fuel consumption Test of engine. China Test, **vol. 47**, no. 1, Sept. 2021, pp. 223-227.

[14] *Z. Sui, H. Y. Wang, Y. Wang.* Vehicle Fuel Consumption and Speed Detection System based on VC Serial Communication. Application of Computer Systems, **vol. 25**, no. 1, Sept. 2016, pp. 63-69.